

A Review of System Delay Compensation Schemes for use in the MI RF System

11/9/2006

T.Berenc, B.Chase, S.Kotz

Introduction: There are various schemes to deal with unavoidable system delays in RF systems. While the schemes presented here are not new, this note reviews them from an engineering perspective to aid the designer in choosing designs and parameters appropriately. The three schemes reviewed here are useful for dealing with delays in RF feedback loops: (1) automatic phase shifting via coherent mixing with delay-separated local oscillators, (2) automatic delay using digital memory and a single clock, and (3) automatic delay using digital memory with two delay-separated clocks.

Automatic Phase Shift via Coherent Mixing with Delay-Separated LO's:

Examples of this technique and its variants have been used in many places; for specific examples see [1], [2], and [3]. The technique is useful for maintaining fixed RF phase relationships in swept RF systems. A block diagram of a specific implementation used here in Fermilab's Main Injector (MI) for maintaining a fixed open-loop RF phase in the Direct RF Feedback loop is shown in Fig. 1.

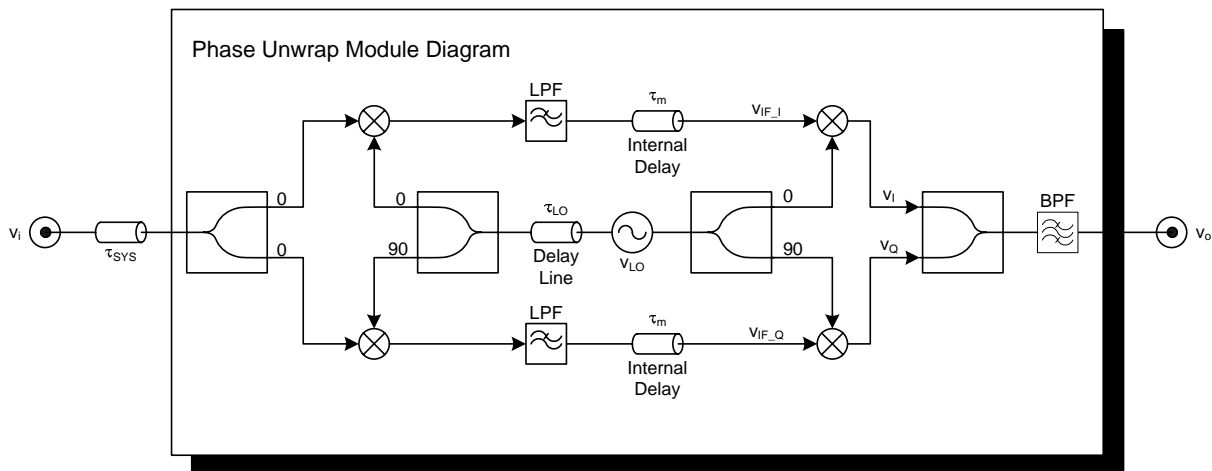


Figure 1: Block diagram of an automatic phase shifter scheme

The purpose of this system is to automatically add a phase shift to a system signal, v_i , to compensate for the phase shift it experiences due to an unavoidable system delay, τ_{sys} . This is essentially accomplished by translating to the signal, via mixing, a comparable phase shift experienced by a local oscillator (LO) signal v_{LO} traveling through a delay τ_{LO} . In essence, the up-converting mixers use an LO signal which leads the LO signal used for down-converting. Thus effectively a positive phase shift is added to the signal to compensate for the negative phase shift experienced through the system delay. The system is still causal in that it does not remove the group delay due to τ_{sys} and τ_m ; it only adds a fixed phase shift. With τ_{LO} almost equal to τ_{sys} , if the LO frequency is swept similar to the frequency sweep of v_i then the phase shift is

automatic and the phase of the output signal, v_o , can be nearly held constant across the frequency sweep. The purpose of using coherent quadrature paths is so that the LO does not have to be synchronized to the system signal for correctly preserving both amplitude and phase information of the original system signal.

From the trigonometric identities and assuming ideal filtering, the corresponding output signal, v_o , for a sinusoidal input signal, v_i , can be expressed as:

$$v_o = \frac{1}{2} \cos(\omega_i t - \omega_i(\tau_m + \tau_{sys}) + \omega_{LO}(\tau_m + \tau_{LO})) \quad (1)$$

where:

- ω_i : the frequency of the system signal v_i
- ω_{RF} : the frequency of system reference signal which is supplied by the LLRF system and used to generate both the LO signal and a reference RF drive signal.
- ω_{IF} : the frequency of the intermediate frequency (IF) signal used to generate the LO signal from the system reference signal.
- ω_{LO} : the frequency of the local oscillator (LO) signal in the automatic phase shifter
- τ_{LO} : a fixed delay used on the LO signal in the automatic phase shifter
- τ_m : the internal delay associated with the automatic phase shifter module
- τ_{sys} : the unavoidable delay associated with RF system

Note that ω_i is only equal to ω_{RF} when the frequency of interest is that of the reference RF drive signal. Otherwise, it represents the frequency associated with any system input, including disturbances which can have any frequency. The second phase term in Eq.1 represents the group delay of the system which cannot be avoided. The third phase term in Eq.1 represents a positive phase offset which varies with ω_{LO} .

The resultant phase shift represented in Eq.1 can be designated as:

$$\phi_o = -\omega_i(\tau_m + \tau_{sys}) + \omega_{LO}(\tau_m + \tau_{LO}) \quad (2)$$

It is clear that ω_{LO} and τ_{LO} can be used to control the resultant phase shift, ϕ_o . For a negative Direct RF feedback system, such as that shown in Fig.2, in which the feedback summing junction already incorporates the sign inversion, one typically desires ϕ_o at the system reference frequency, $\omega_i = \omega_{RF}$, to be zero so that the feedback loop tries to force the system to follow the input reference in both magnitude and phase. There are, however, situations in which this phase shift may be tuned unequal to zero; i.e. for trying to make the closed loop transfer function symmetric about the system reference frequency as suggested in [4]. To parameterize the tuning, the frequency at which the calibration/tuning is done is designated as ω_{RF_tune} and the resultant

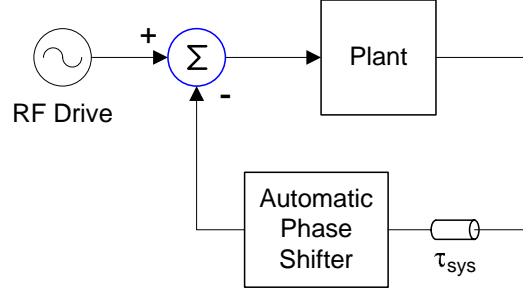


Figure 2: Simplified block diagram of a Direct RF Feedback system with system delay

phase shift at the tuning frequency is designated as ϕ_{o_tune} . Thus, the adjustment of ω_{LO} and τ_{LO} is performed to achieve:

$$\phi_{o_tune} = \phi_o \Big|_{\omega_i = \omega_{RF_tune}} = \omega_{LO}(\tau_m + \tau_{LO}) - \omega_{RF_tune}(\tau_m + \tau_{sys}) \quad (3)$$

For the special case of $\phi_{o_tune} = 0$, it is obvious that perfect cancellation can be achieved at any system reference frequency, ω_{RF} , if $\omega_{LO} = \omega_{RF}$ and $\tau_{LO} = \tau_{sys}$. This implies that the LO frequency, ω_{LO} , is swept to follow ω_{RF} . However, this situation is not always chosen due to self-mixing terms in the down-converting and up-converting stages causing errors associated with the LO ‘leakage’ which would appear at the RF drive frequency. Instead, a fixed intermediate frequency (IF) signal is used such that $\omega_{LO} = \omega_{RF} - \omega_{IF}$. In this situation, τ_{LO} may not necessarily be equal to τ_{sys} . Rather it is chosen to compensate for the additional phase term due to the choice of using an IF. Thus, the characterizing equation for τ_{LO} is expressed as:

$$\tau_{LO} = \frac{\phi_{o_tune} + \omega_{RF_tune}\tau_{sys} + \omega_{IF}\tau_m}{(\omega_{RF_tune} - \omega_{IF})} \quad (4)$$

The choice of the IF frequency is a compromise between pushing the LO frequency far enough away from the RF frequency to relax the output bandpass filter (BPF) requirements and not pushing it out too far that it defeats the automatic phase shifter’s ability to compensate across a large RF frequency sweep. Relaxing the output BPF requirements reduces the amount of group delay that the filter introduces. In addition, using a high IF frequency also pushes the image sideband, which is twice as far from the RF frequency as the LO frequency is, further away from the RF frequency. Thus, the BPF can easily suppress the image sideband. On the other hand, the higher the IF frequency, the less the phase shifter can automatically adjust the phase over a large RF frequency sweep.

Summarizing the resultant phase shift of the system delay plus the automatic phase shifter under the tuning of Eq.4, Eq.2 becomes:

$$\phi_o = -\omega_i(\tau_m + \tau_{sys}) + (\omega_{RF} - \omega_{IF}) \left[\tau_m + \frac{\phi_{o_tune} + \omega_{RF_tune}\tau_{sys} + \omega_{IF}\tau_m}{(\omega_{RF_tune} - \omega_{IF})} \right] \quad (5)$$

Keep in mind that the first term represents a pure delay of $\tau_m + \tau_{sys}$ while the second term represents a fixed phase offset at a particular RF system reference frequency ω_{RF} .

The parameters of this system are:

- ω_i : the frequency of the system signal of interest
- ω_{RF} : the system reference signal frequency, supplied by the LLRF system. The system reference signal is the signal which is used to generate the LO signal
- ω_{IF} : the intermediate frequency (IF) used to generate the LO signal from the system reference signal for the automatic phase shifter
- ω_{LO} : the local oscillator (LO) frequency used in the up-convert and down-convert processes
- τ_{LO} : the delay used on the LO signal of the automatic phase shifter
- τ_m : the delay associated with the automatic phase shifter module
- τ_{sys} : the unavoidable delay associated with RF system
- ω_{RF_tune} : the RF drive frequency at which the tuning of τ_{LO} is done
- ϕ_o : the resultant phase angle of the automatic phase shift process including the unavoidable system delay
- ϕ_{o_tune} : the resultant phase angle of at the τ_{LO} tuning point

The specific implementation in the MI's Direct RF Feedback loop can be used to understand the design tradeoffs. The MI RF frequency sweep is from 52.8114 MHz to 53.104 MHz. Originally the Direct RF Feedback's automatic phase shifter used a 3.8114 MHz IF frequency with no output BPF. This resulted in an LO frequency sweep from 49 MHz to 49.2926 MHz. The unavoidable LO leakage appeared to the error summing junction of Fig.2 as a system disturbance. Even though the RF cavities have only an ~15kHz bandwidth, the bandwidth of the RF tetrode amplifier chain is on the order of 10MHz. Thus, the cavity could filter this component out but the amplifier chain could not; hence real power could be wasted in the amplifier chain. At high enough feedback gains, the 49 MHz LO leakage component could be at equal or greater amplitude than the RF drive frequency component. As much as twice the tetrode DC anode current was needed with direct RF feedback to make the same cavity voltage as without direct RF feedback. Figure 3 depicts this original problem by showing the required tetrode DC anode current for various RF feedback gains while making the same cavity gap voltage. The spectrum of the amplifier drive signal is shown in Fig.4.

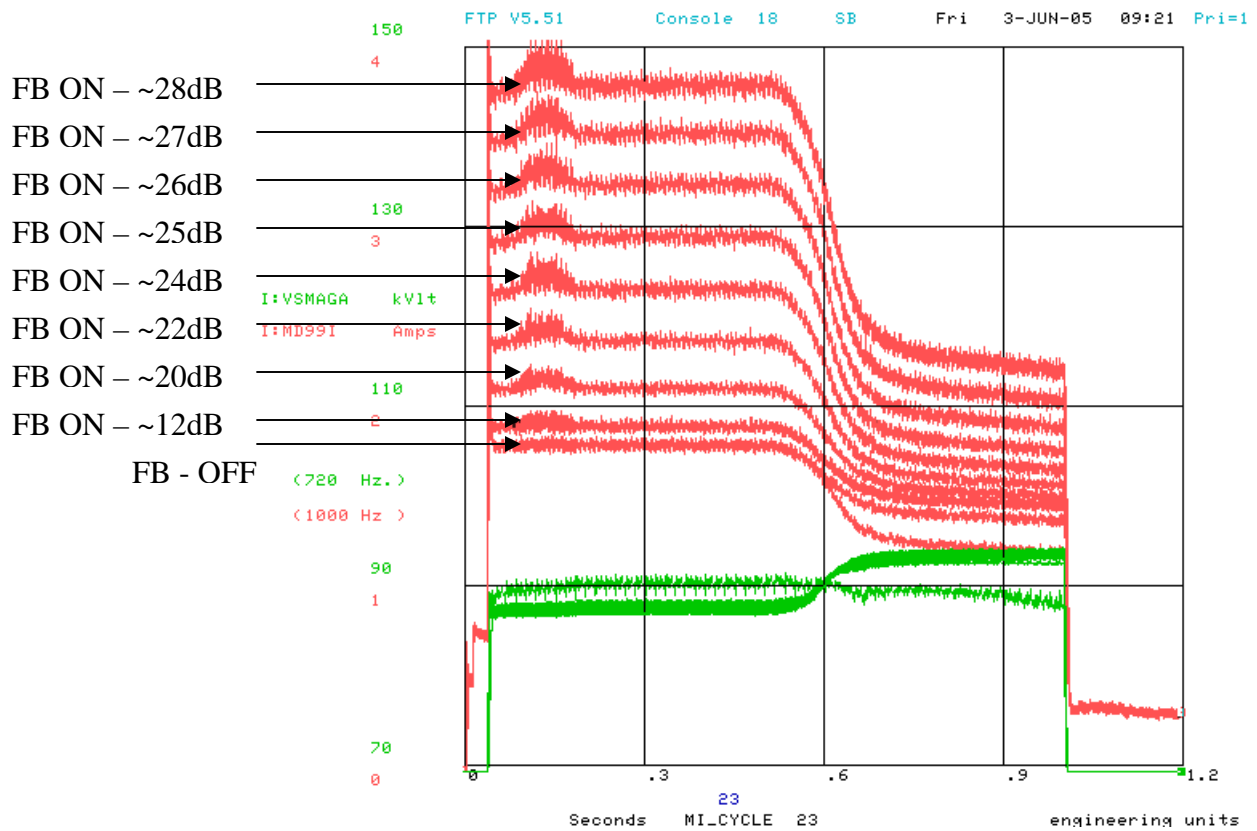


Figure 3: RF tetrode amplifier DC Anode current (I:MD99I) across a typical MI operational cycle without any beam for various Direct RF Feedback gains for ~same cavity gap voltage (I:VSMAGA) between all conditions while using the original 3.8114 MHz IF without an output BPF. The decrease in anode current across the cycle is due to the increase in cavity Q across the RF frequency sweep.

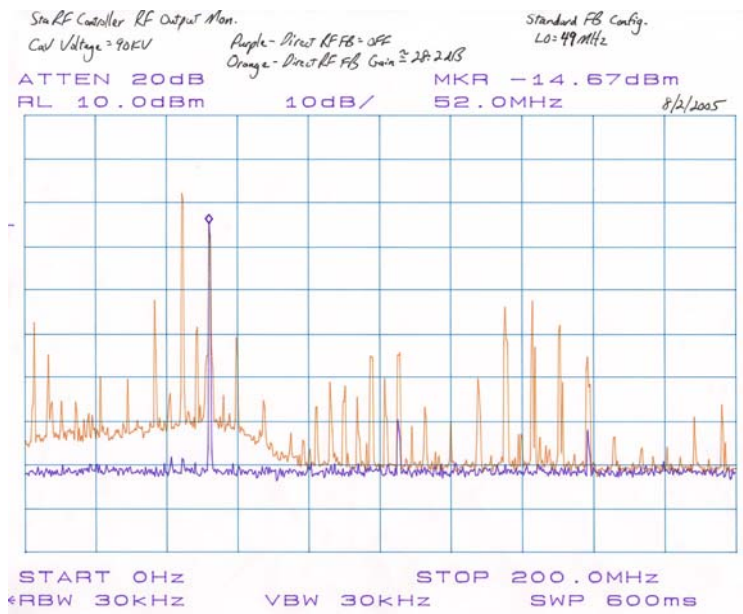


Figure 4: RF drive signal for original 3.8114 MHz IF without output BPF for without FB (purple trace) and with 28 dB of Direct RF Feedback (orange trace). The largest component with FB on is the LO leakage at 49 MHz. The other components with FB on are cross products from the mixing processes in the automatic phase shifter.

The design was subsequently changed to an IF frequency of 8 MHz and included an output BPF with a bandwidth of 13 MHz. The previous measurements were repeated for this configuration and are shown in Fig. 5 and Fig.6.

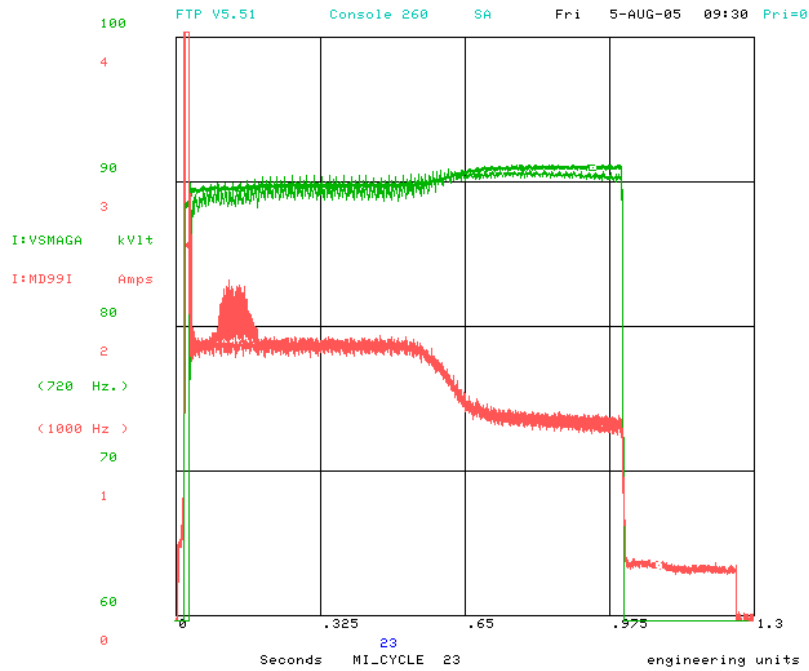


Figure 5: Modified design: 8 MHz IF and 13 MHz wide BPF. RF tetrode amplifier DC Anode current (I:MD99I) across a typical MI operational cycle without any beam under conditions of both (1) without direct RF Feedback and (2) with 28 dB of Direct RF Feedback gain for ~same cavity gap voltage (I:VSMAGA). Again the decrease in anode current across the cycle is due to the increase in cavity Q across the RF frequency sweep. Note the only change in anode current between the two conditions is during the slipping portion of the cycle at ~0.11 seconds. This is due to the frequency/phase change associated with the slip-stacking process. Compare to Fig. 3.

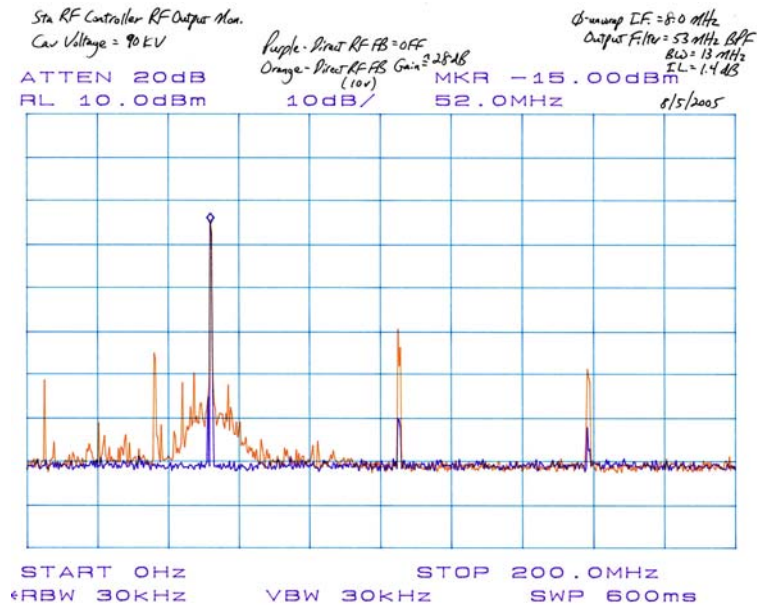


Figure 6: RF drive signal for modified design with an 8 MHz IF and a 13 MHz wide BPF for without FB (purple trace) and with 28 dB of Direct RF Feedback (orange trace) for comparison to Fig. 4.

Figure 7 displays the compromise made in the automatic phase shifter's ability to compensate across the operating RF frequency sweep for the increased IF frequency choice. It is merely a graph of Eq. 5 with $\phi_{o_tune} = 0$, $\omega_{RF_tune} = 2\pi \cdot 52.9577\text{MHz}$ (which is the median of the MI frequency range), $\omega_i = \omega_{RF}$, $\tau_{sys} = 450\text{ nsec}$, and $\tau_m = 16\text{ nsec}$.

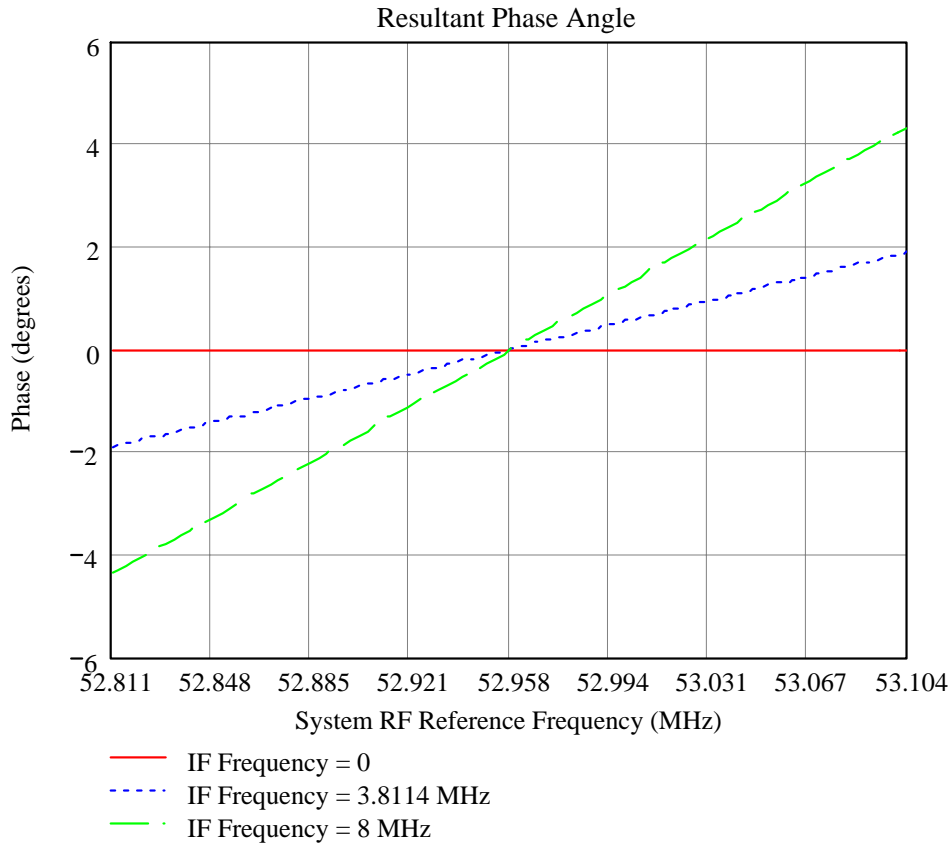


Figure 7: Resultant phase angle of the system delay + automatic phase shifter for the MI Direct RF Feedback system for 3 different choices of IF frequency: (red) 0 MHz IF, (blue) 3.8114 MHz IF, (green) 8 MHz IF.

Digital Automatic Delay using a Single Clock

The second scheme reviewed in this note is to incorporate a digital memory which delays a signal by an integer number of a sampling clock period which is synchronized with the RF system reference frequency. An example of this scheme is found in the MI Feed Forward beam loading compensation system in which it is desired to generate a one-turn delay which changes with the RF frequency sweep. A representation of this system is shown in Fig. 8.

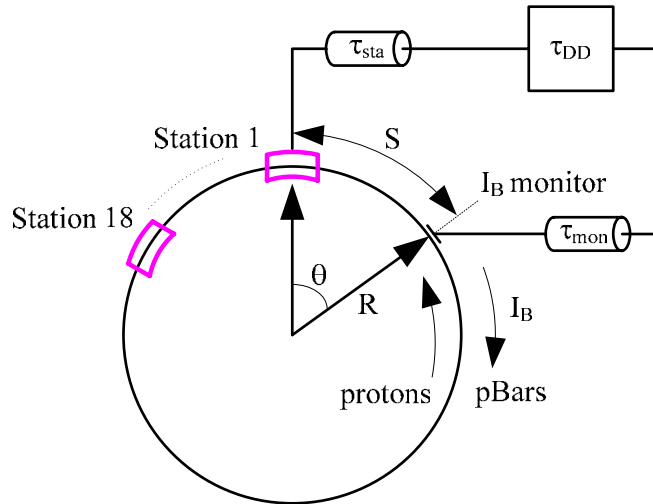


Figure 8: Block diagram of the MI Feed-Forward system with a digital automatic delay, τ_{DD} .

In Fig. 8 a beam current monitor samples the beam current and is delayed so as to meet and cancel with the beam current when the beam passes through each cavity; hence the name feed-forward from control system terminology. The beam current monitor is located arclength S away from station 1. A delay cable, represented as τ_{mon} , connects the beam current monitor to a digital delay, τ_{DD} , which is common to all 18 stations. A fanout system then provides a separate delay, τ_{sta} , to each station. From an aerial view of the MI, protons travel counterclockwise while anti-protons travel clockwise. Thus, there is a separate feed forward fanout system for both protons and pBars. For protons, the beam sees station 1 first, thus the station cables, τ_{sta} , are successively longer from station 1 to 18. For pBars, the situation is reversed; the cables are successively longer from station 18 to 1. However, since station 1 is closest to the fanout system in the MI control room, the first cable length (station 1/18 for protons/pBars respectively) is different in both cases.

To understand the details of the successive lengths of the fanout system, a simple review of cavity placement along a synchrotron ring is helpful:

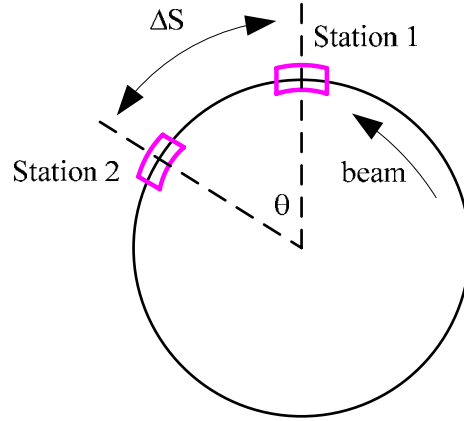


Figure 9: Diagram for discussion of cavity placement along a synchrotron

Referring to Fig.9, assume that station 1 is operating with a time-varying voltage $V\cos(\omega_{RF} t)$. In order for the beam to see the same voltage in station 2 that it sees when crossing station 1, the voltage at station 2 should be delayed from station 1 by the beam transit delay between the two stations, $\Delta\tau_S$. Thus the voltage at station 2 can be written as $V\cos(\omega_{RF}(t - \Delta\tau_S))$. The beam transit time between the two stations can be expressed as a fraction of the beam revolution period, τ_{rev} , as $\Delta\tau_S = \frac{\Delta S}{C} \cdot \tau_{rev}$; where C is the ring circumference and ΔS is the arclength between the two stations. Since the RF frequency is related to the revolution frequency through the machine harmonic number, h , $\omega_{RF} \cdot \Delta\tau_S = 2\pi \cdot h \cdot \frac{\Delta S}{C}$ and the voltage at station 2 can be expressed as $V\cos\left(\omega_{RF} t - 2\pi h \frac{\Delta S}{C}\right)$. Thus, the phase difference between the two stations is constant for all RF frequencies. This is really no surprise due to the circular geometry. The station spacing is thus chosen such that the RF phasing between stations can be conveniently generated. In the MI the nominal station to station spacing is chosen such that the nominal RF phasing between stations is 180 degrees at all RF frequencies, or $\frac{\Delta S}{C} = \frac{1}{2h}$. Thus, the nominal time delay between stations can be considered to be $\frac{1}{2}$ an RF period irrespective of RF frequency. There are 3 locations in the MI where the consecutive station spacing is larger than the nominal distance; (1) between stations 4 and 5 the spacing is three times the nominal distance, (2) between stations 9 and 10 the spacing is twice the nominal distance, and (3) between stations 14 and 15 the spacing is three times the nominal distance. Thus the total spacing between stations 1 and 18 is $22 \cdot \frac{\Delta S}{C}$.

Since the fanout cables to each station, represented as τ_{sta} in Fig.8, are fixed, the fanout cable delays can only match the beam transit time at one RF operating frequency. The choice of this operating frequency for the MI feed forward fanout installation was 53.104 MHz. Thus, the nominal time delay difference, $\Delta\tau_{sta}$, between the feed forward fanout station cables is

$\frac{1}{2 \cdot 53.104 \text{ MHz}}$. The cable lengths are successively longer/shorter for protons/pBars. Due to the cavity spacing discussed above, the difference in cable delay: (1) between stations 4 and 5 is three times the nominal delay, (2) between stations 9 and 10 is twice the nominal delay, and (3) between stations 14 and 15 is three times the nominal delay. Again, since station 1 is closest to the MI control room the shortest fanout cable delay for protons is to station 1 and is equal to 4 RF periods at 53.104 MHz. Since station 18 is the furthest from the MI control room, the shortest fanout cable for pBars is to station 18 and is equal to 15 RF periods at 53.104 MHz.

Referring back to Fig.8, and assuming that a sign reversal is provided somewhere within the feed forward system, the objective for each station is that:

$$\tau_S + \tau_{mon} + \tau_{DD} + \tau_{sta} = \tau_{rev} \quad (6)$$

where:

- $\tau_S = \pm \frac{S}{C} \cdot \tau_{rev}$: the beam transit time between the station and the beam current monitor. It is positive/negative if the beam sees the station before/after the monitor. Thus for the MI configuration of Fig.8, it is positive for pBars and negative for protons.
- τ_{mon} : the delay associated with the single cable connecting the beam current monitor to the feed forward electronics. For this discussion it also includes the fixed delay associated with the feed-forward electronics which is common to all stations.
- τ_{DD} : the digital delay generated by the sampling + digital memory electronics
- τ_{sta} : the feed-forward fanout cable between the common feed-forward electronics and a unique station. Note that it is different for each station as discussed above.
- τ_{rev} : the beam revolution period or ‘one-turn’ delay.

Note that τ_S and τ_{rev} both change with the RF frequency sweep and that τ_{mon} and τ_{sta} are fixed delays. Furthermore, τ_S and τ_{sta} are unique to each station. Thus, it is clear that, ideally, τ_{DD} should be unique for each station. The present feed forward system uses a τ_{DD} that is common to all stations. Thus, there is only 1 station for which Eq.6 can be exact. Furthermore, the way in which τ_{DD} is generated can also cause errors.

Presently, τ_{DD} is generated by sampling the beam current monitor signal with an ADC using a sampling clock, f_{CLK} , then delaying the signal with an N (an integer) cell first-in first-out (FIFO) memory, and finally regenerating an analog signal with an output DAC. Due to the existing hardware limit on the sampling clock, the beam current monitor signal is downconverted into separate I and Q paths to a lower IF frequency, f_{IF} , before being digitally sampled. After digitally delaying the signal, the signal is reconstructed by upconverting back to the original RF frequency. The ideal defining equation for τ_{DD} thus becomes,

$$\tau_{DD} = \frac{N}{f_{CLK}} = \tau_{rev} \cdot \left(1 - \frac{S}{C}\right) - \tau_{mon} - \tau_{sta} \quad (7)$$

It is clear that if $S = \tau_{mon} = \tau_{sta} = 0$ the natural choice for f_{CLK} would be $N \cdot f_{rev}$ with N chosen properly such that the sampling frequency is appropriate for the signal bandwidth. Thus f_{CLK} should be synchronized to the RF frequency sweep. Clearly this is not the situation due to the unavoidable delays τ_s and τ_{sta} and the distance S separating the cavity and the beam current monitor. Instead f_{CLK} and N have to be chosen to best satisfy Eq.7 across the RF frequency sweep. This means that: (1) the change in τ_{DD} should track the change in τ_{rev} across the RF frequency sweep and (2) the absolute value of τ_{DD} has to be correct to properly combine with the existing fixed delays τ_s and τ_{sta} to satisfy Eq.7. Thus, a natural choice for generating f_{CLK} is for it to still be related to the RF frequency; i.e. $f_{CLK} = f_{RF} - f_{CLK_IF}$.

Since there are two free parameters that can be adjusted for the design, f_{CLK_IF} and N , two independent equations can be written and solved for these parameters. A third parameter, τ_{mon} , can be used for fine tuning adjustments. A natural choice for these two equations would be Eq.7 at two different RF frequencies; at an initial frequency, $f_{RF_initial}$, (i.e. at injection) and at a final frequency, f_{RF_final} , (i.e. at extraction). These two equations can be written as:

$$\frac{h}{f_{RF_initial}} \cdot N + \left[\frac{h}{f_{RF_initial}} \cdot \left(1 - \frac{S}{C}\right) - (\tau_{mon} + \tau_{sta}) \right] \cdot f_{CLK_IF} = \left[\left(1 - \frac{S}{C}\right) \cdot h - (\tau_{mon} + \tau_{sta}) \cdot f_{RF_initial} \right] \quad (8a)$$

$$\frac{h}{f_{RF_final}} \cdot N + \left[\frac{h}{f_{RF_final}} \cdot \left(1 - \frac{S}{C}\right) - (\tau_{mon} + \tau_{sta}) \right] \cdot f_{CLK_IF} = \left[\left(1 - \frac{S}{C}\right) \cdot h - (\tau_{mon} + \tau_{sta}) \cdot f_{RF_final} \right] \quad (8b)$$

Eq.8 is a simple system of the form:

$$A_{11} \cdot N + A_{12} \cdot f_{CLK_IF} = D_{11} \quad (9a)$$

$$A_{21} \cdot N + A_{22} \cdot f_{CLK_IF} = D_{21} \quad (9a)$$

With solutions:

$$N = \frac{\begin{vmatrix} D_{11} & A_{12} \\ D_{21} & A_{22} \end{vmatrix}}{\begin{vmatrix} A_{11} & A_{12} \\ A_{21} & A_{22} \end{vmatrix}} \quad (10a) \quad \text{and} \quad f_{CLK_IF} = \frac{\begin{vmatrix} A_{11} & D_{11} \\ A_{21} & D_{21} \end{vmatrix}}{\begin{vmatrix} A_{11} & A_{12} \\ A_{21} & A_{22} \end{vmatrix}} \quad (10b)$$

To satisfy the constraint that N must be an integer, the solution given by Eq.10a can be rounded to the nearest integer.

Since the digital delay is common to all stations, the above equations can only be solved for one station. The errors associated with the other stations can be investigated by forming the difference of Eq.6 for two different stations, m and n , and call this the error, τ_{delay_error} , in realizing a ‘one-turn’ delay.

$$\tau_{delay_error} = \left(\frac{S_m}{C} - \frac{S_n}{C} \right) \cdot \frac{h}{f_{RF}} + (\tau_{sta\ m} - \tau_{sta\ n}) \quad (11a)$$

Since the theoretical fanout cabling configuration was chosen to be matched at 53.104 MHz and is configured as discussed above, Eq.11a can be rewritten as:

$$\tau_{delay_error} = h \cdot \left(\frac{S_m - S_n}{C} \right) \left(\frac{1}{f_{RF}} - \frac{1}{53.104MHz} \right) \quad (11b)$$

Thus, the theoretical error between stations is zero at extraction, $f_{RF} = 53.104MHz$; whereas theoretically the error between any two stations is greatest at injection, $f_{RF} = 52.8114MHz$. The worst error would be between the two stations that are separated the furthest; stations 1 and 18, for which $\left(\frac{S_m - S_n}{C} \right) = \frac{11}{h}$. The worst error is $11 \cdot \left(\frac{1}{52.8114MHz} - \frac{1}{53.104MHz} \right) = 1.148$ nsec corresponding to a phase error of 21.8 deg at 52.8114 MHz.

Assuming that one was trying to counteract the beam current with a signal that was 21.8 deg out of phase from the ideal compensating signal, one would attempt to make a magnitude correction to compensate for the phase error. This can be viewed theoretically by looking at the resultant of two sinusoids that are separated by 180 deg except for a phase error ϕ_{delay_error} :

$$I_R \cos(\omega t + \phi_R) = I_{FF} \cos(\omega t + \phi_{delay_error}) - I_{Beam} \cos(\omega t) \quad (12)$$

where $I_R = \sqrt{I_{FF}^2 + I_{Beam}^2 - 2I_{FF}I_{Beam} \cos(\phi_{delay_error})}$ would be the resultant current in the cavity after trying to counteract the beam current, I_{Beam} , with the feed-forward current, I_{FF} . Taking the derivative of I_R with respect to I_{FF} to find the value of I_{FF} that minimizes I_R results in $I_{FF} = I_{Beam} \cdot \cos \phi_{delay_error}$ and $I_R = I_B \cdot \sqrt{1 - \cos^2 \phi_{delay_error}}$. For the 21.8 deg phase error found above, this implies that, the compensation could only achieve a resultant vector of 37.1% of the beam current, or only a 62.9% reduction. This assumes that the system is tuned perfectly for station 1 while taking the largest error at station 18. Of course, after reviewing these errors, it would be prudent to perform the digital delay tuning (solution to Eq.8) at a station somewhere in the middle to reduce the error to half this value at the two stations furthest from the middle.

To summarize the above for the specific MI feed forward configuration, we assume the following:

Table 1: Assumed nominal MI Feed Forward system parameters

parameter	value	Note
τ_{mon}	721.531 nsec	common beam current monitor delay cable
$\tau_{\text{sta 1}}$	75.323nsec/282.464nsec	Sta 1 feed forward cable delay for protons/pBars
h	588	machine harmonic number
C	3319.4 m	Main Injector Circumference
S_1/C	-/+ 11.887 m	the beam monitor is -/+ 11.887m from sta1 for protons/pBars
f_{initial}	52.8114 MHz	injection frequency
f_{final}	53.104 MHz	extraction frequency

For the nominal parameters given in Table 1, the solution to Eq.8 gives $N = 509$ and $f_{\text{CLK_IF}} = 3.761\text{MHz}$. The actual values used in the system are $N = 494$ and $f_{\text{CLK_IF}} = 3.8114\text{MHz}$. The difference could be due to a variety of practical concerns; i.e. differences in the assumed nominal parameters given above, non-ideal performance of the digital delay hardware, or other non-ideal practical parameters not modeled in this simple analysis. The following figures give the resultant error in the resultant one-turn delay at stations 1, 9, and 18 for two scenarios: (1) Fig.10 assumes station 1 is the reference station for protons (solution is $N = 509$ and $f_{\text{CLK_IF}} = 3.761\text{MHz}$), and (2) Fig.11 assumes station 9 is the reference station for protons ((solution is $N = 514$ and $f_{\text{CLK_IF}} = 3.727\text{MHz}$),

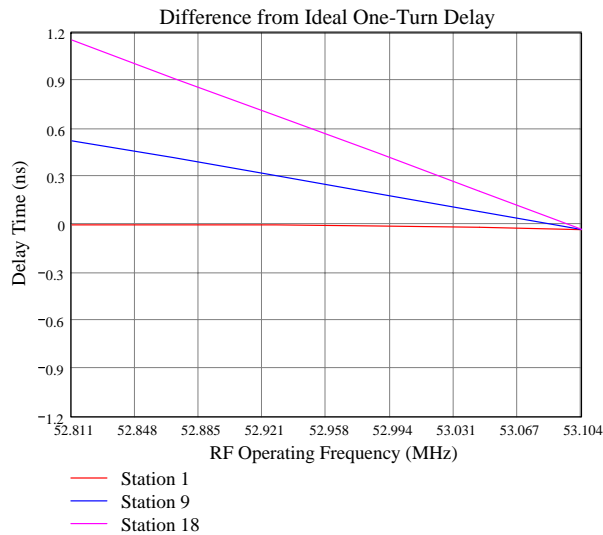


Figure 11: Difference from the ideal one-turn delay at stations 1, 9, and 18 assuming that station 1 is used as the tuning reference station. The theoretical solution to Eq.8 for this scenario is $N = 509$ and $f_{\text{CLK_IF}} = 3.761\text{MHz}$

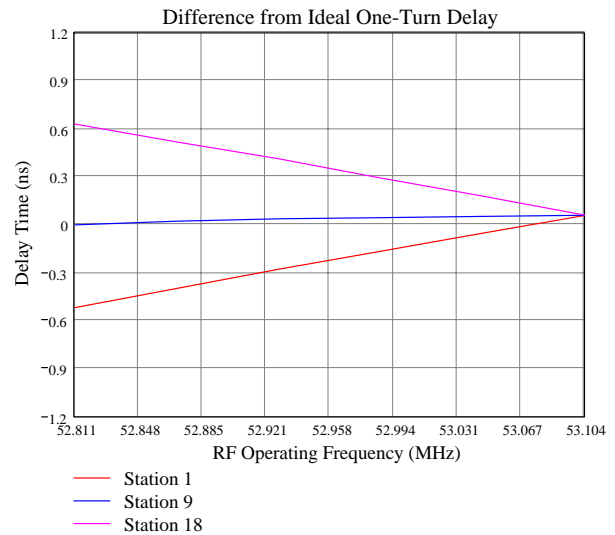


Figure 10: Difference from the ideal one-turn delay at stations 1, 9, and 18 assuming that station 9 is used as the tuning reference station. The theoretical solution to Eq.8 for this scenario is $N = 514$ and $f_{\text{CLK_IF}} = 3.727\text{MHz}$

Digital Automatic Delay using Delay-Separated FIFO Clocks

The third scheme reviewed in this note is a digital delay scheme similar to the one just described; however, instead of using a single clock for the digital FIFO, the FIFO input clock is delayed with respect to the FIFO output clock by an amount τ_{CLK} as shown in Fig. 12.

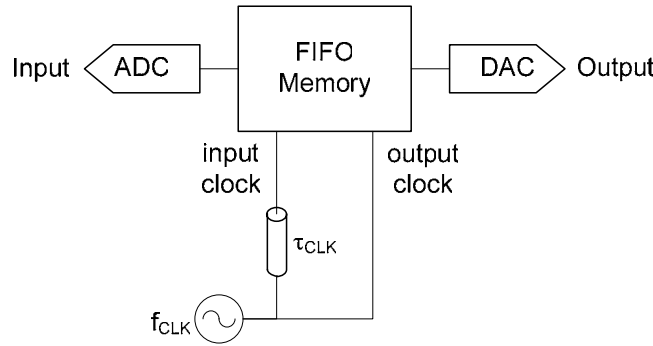


Figure 12: Simple block diagram of dual clocked FIFO

The architecture is analogous to an asynchronous dual-port memory FIFO. The technique applied to a ‘one-turn’ delay comb filter RF feedback system is found in [5]. This scheme is not yet used in MI, but is suggested for use for the comb filter design as part of the MI RF upgrades for Proton Plan. Although the fine details of its operation will have to be engineered, the simplistic view of its operation is as follows:

A common FIFO design is to use a write pointer for writing the input signal to memory and a read pointer to read the memory for output. The length of the FIFO is n_{FIFO} (an integer) cells. In a simple design for which $\tau_{CLK} = 0$, the read and write pointers start out in the same location with the read operation taking place first. When the end of the FIFO memory is reached, the pointers wrap around to the beginning of the FIFO memory; thus creating a circular memory. Since the read operation takes place first, the read pointer doesn’t return to the first write pointer location until n_{FIFO} cells later. If the pointer clocks are clocked at $T_{CLK} = \frac{1}{f_{CLK}}$, then a

$n_{FIFO} \cdot T_{CLK}$ delay is realized between the input and the output; neglecting internal latency and group delays which can be lumped into an external delay term to be discussed shortly. Thus, to realize a ‘one-turn’ delay, $T_{rev} = \frac{1}{f_{rev}}$, the required number of cells is obviously $n_{FIFO} = \frac{T_{CLK}}{T_{rev}}$.

And thus, since n_{FIFO} is an integer, the sampling clock is harmonically related to the revolution frequency.

This simple picture breaks down once the delay is inserted into a practical system which has an unavoidable system delay, τ_{sys} , as shown in Fig. 13. This is similar to Fig.2 where the automatic phase shifter is replaced with the digital FIFO delay. The purpose is to realize a one-turn delay so that the feedback system can have large gain near the revolution harmonics to reduce coupled bunch growth rates and transient beam loading. By making a one-turn delay, the open-loop phase at the revolution harmonics is adjusted such that the loop can be closed in a stable manner. For the pioneering use of the one-turn delay comb filter RF feedback and a discussion of the purpose of the one-turn delay see [1].

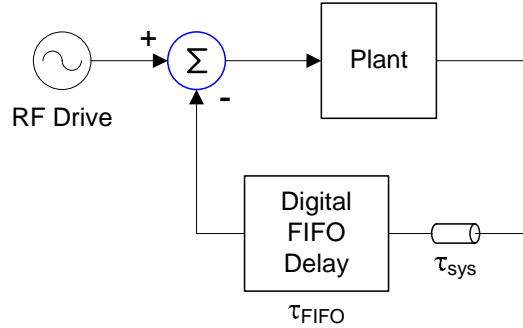


Figure 13: Digital FIFO delay used in a system with unavoidable delay τ_{sys}

In this situation, the total delay of the FIFO plus the unavoidable delay τ_{sys} needs to be one-turn. Thus the FIFO delay, τ_{FIFO} , has to be less than a turn; $\tau_{FIFO} = T_{rev} - \tau_{sys}$. Theoretically, if the FIFO input clock delay, τ_{CLK} , of Fig. 12 is set equal to τ_{sys} , then the output pointer will lead the input pointer by τ_{sys} seconds; thereby realizing the less than one turn delay. There will be practical design details to deal with to ensure that the pointers are initialized properly and that metastability is avoided during the asynchronous operation during RF frequency sweeps.

Conclusion

Three schemes to deal with unavoidable system delays in RF systems have been reviewed with particular detail to the schemes used in the MI RF system. The third scheme has not yet been incorporated into the MI but is suggested for use for the comb filter of the MI RF upgrade for Proton Plan. The details of this scheme need to be engineered for it to be stable and reliable.

References

- [1] D.Boussard, G.Lambert, "Reduction of the Apparent Impedance of Wide Band Accelerating Cavities by RF Feedback", IEEE Transactions on Nuclear Science, Vol. NS-30, No.4, August 1983.
- [2] T.Miyanaga, "Signal Generation System (Synthesizer System)", Michigan State University RF Note #83, May 6, 1982.
- [3] J.Dey, J.Steimel, J.Reid, "Narrowband Beam Loading Compensation in the Fermilab Main Injector Accelerating Cavities", IEEE 2001 Particle Accelerator Conference, pp.876-878.
- [4] F.Pedersen, "RF Cavity Feedback", SLAC Report 08, BFactory 92-025, 1991, <http://www.slac.stanford.edu/pubs/slacreports/reports08/bfac92-025.pdf>.
- [5] F.Blas, R.Garoby, "Design and Operational Results of a 'One-turn-delay Feedback' for Beam Loading Compensation of the CERN PS Ferrite Cavities", IEEE 1991 Particle Accelerator Conference, 91CH3038-7, pp1398-1400.